ANALYSIS OF CRITICAL FLIGHT REGIMES OF UNMANNED AERIAL VEHICLES (UAVS)

Vasile PRISACARIU

"Henri Coandă" Air Force Academy, Brasov, Romania

The aerodynamics of lifting surfaces has undergone a significant evolution determined both by conceptual perspective and by the materials used and related technologies. Accelerating this evolution was also possible due to the use of numerical modeling tools that offered and still offer computational speeds that were not possible a century ago. The constructive concepts of unmanned aerial vehicles (UAVs) offer complex aerodynamic approaches in terms of flight regimes, providing research opportunities on design and manufacturing limitations with direct effects on flight safety.

The article wants to highlight critical flight from the perspective of using a freeware tool. The 2D aerodynamic analysis cases of the aerodynamic and 3D profiles of the simple lifting surfaces offer a perspective on the calculation possibilities both through the multiple case studies offered and the expressed results.

Key words: *UAV, aerodynamic analysis, XFLR5, critical regimes, flight instability*

Symbols and acronyms

C_{m_α} C_{n_β} C_{l_β}	*- derivates of static stability*	C_z, C_x	*- aerodinamyc coefficients*
α, *AOA, alpha*	*- angle of attack*	C_p	*-pressurre coefficient*
S	*-lifting surface*	*b*	*-span*
AR	*-aspect ratio*	*c*	*- airfoil chord*
MAC	*-main aerodynamic chord*	*l*	*-lenght*
u_o	*-perturbation speed*	Ω	*-rotation rate*

1. THEORETICAL ASPECTS

1.1. Introduction

The maneuverability of a UAV is limited, outside these limits the UAV is in the area of critical flight regimes (uncontrollable regimes with loss of stability) where the actions of UAV operators may prevent or cause the development of instability depending on the flight mode (assisted or free/acrobatic). Due to external disturbances or the desire to increase the maneuverability of an aircraft, it inevitably results in entering unstable regimes where aerodynamic characteristics are seriously affected, critical regimes or unstable modes of movement being serious safety challenges, [1, 2, 3, 4].

Extreme situations are possible in flight due to external causes, for example: gusts, poor piloting, the aircraft may move to critical or supercritical angel of attack, moments when there are variations and changes of direction of forces and aerodynamic moments which can lead to flight incidents. Cases of loss of static stability are defined by the three derivatives of static stability ($C_{m_\alpha}, C_{n_\beta}, C_{l_\beta}$), and which depend on the flight regime of the aircraft, so that in some flight regimes there is a significant decrease in static stability, sometimes leading to complete loss of its.

According to the literature [4, 5] all critical regimes can be divided into two categories depending on the dangerous behavior of the airplane. The first category of critical regimes appear when the margin of stability is performed and unstable modes of movement begin to develop (slow or sudden loss of stability) where we have an evolution on a controllable or uncontrollable trajectory, such situations are speed limit flights or high-speed maneuvering flights. The second category is stable flight regimes with supercritical values of parameters (AoA and rotation speed), such as evolutions in autorotation or inertial rotation, see figure 1.

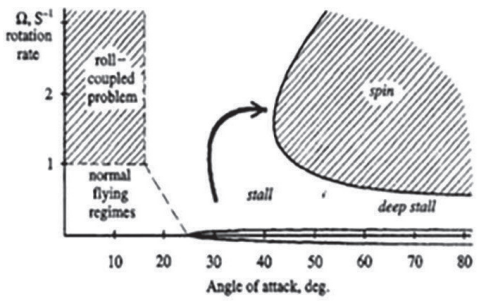

Fig. 1 Areas of critical flight regimes

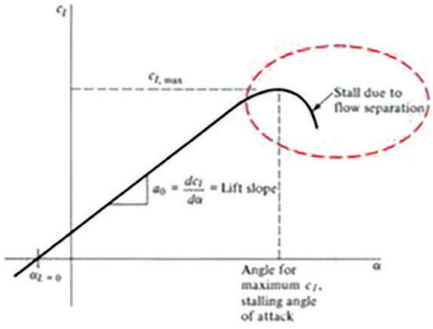

Fig. 2 Critical angle of attack (α)

The current state of research [6, 7, 8] reveals many of forms of loss of stability (forms dependent on the flight speed limit), as follows: sudden increase in angle of attack (AoA) due to the nonlinearity of the moment of dive; self-oscillating movement at large angles of attack, figure 2 (due to detachment of the boundary layer from the upper surface); self-harness; divergent increase of the lateral tilt angle due to the asymmetrical rolling moment (eg asymmetric propulsion or very high AoA); divergent increase of the sliding angle due to aperiodic instability or asymmetric aerodynamic moments; oscillating roll and turn movements at high angles of attack; loss of stability in the maneuvering flight on the trajectory. Here are some characteristic situations of static instabilities, of changing the signs of the three derivatives, which necessarily determines the loss of the (dynamic) stability of the plane, [9].

1.2. Cases of loss of flight stability

1.2.1. Longitudinal instability (self-increase pitch moment)

Longitudinal instability in relation to the angle of attack (AoA) - commonly referred to as self-increase pitch moment, can occur in some high-speed aircraft in the field of transonic velocities; however, most often, self-increase pitch moment takes place in flights with high angles of attack, see figure 4. The curve $C_m=C_m(\alpha)$ of an airplane predisposed to self-increase pitch moment has the appearance represented in figure 3, [9].

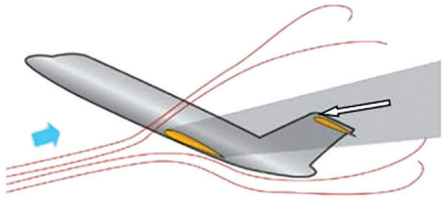

Fig. 3 Horizontal tail top

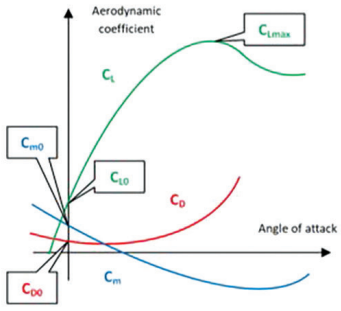

Fig. 4 C_m versus AoA (α) for self-increase pitch moment

the slope of the curve is negative, we have:

$$C_{m_\alpha} = \frac{\partial C_m}{\partial \alpha} < 0 \qquad (1)$$

The airplane is statically stable longitudinally, which also implies a dynamic stability in relation to the angle of attack. At high AoA, however, in the vicinity of critical AoA, the slope of the curve changes its sign, $C_{m_\alpha} > 0$ and The plane becomes unstable. The airplanes most exposed to self-increase pitch moment at high AoA are those that have the horizontal tail top, see figure 3.

In this case, due to the huge deflection of the current near the horizontal tail, its drag force becomes significant in relation to the lift and, consequently, the moment of pitch of the horizontal tail to the aircraft mass center can become destabilizing. In the usual cases of low flight incidences, only the pitch of the horizontal tail lift was taken into account:

The phenomenon is more accentuated in airplanes with reduced aspect ratio of wing, given the rapid increase of the deflection of the downstream current at high AoA in the case of these wings.

Static instability leads to loss of stability of the fast mode of longitudinal disturbing motion, as this is a short-period oscillating mode, the only sure measure of correction is to equip of aircraft that have this tendency with automatic pitch stabilizers (autopilot).

Figure 5 shows numerical benchmarks of the pitching moment coefficient for a number of aircraft types, and Figure 6 shows the pitching moment coefficient values of the building components of an aircraft.

$$\Delta C_m = -\vec{V} C_{z_2} \tag{2}$$

where V – tail volume

C_{z2} *– lift coefficient of the horizontal tail*

at high AoA, in the above conditions, the contribution of the drag force of the horizontal tail must be taken into account:

$$\Delta C_m = \frac{Z_2 S_2}{CS} C_{x_2} - \frac{l S_2}{cS} C_{z_2} \quad \text{where} \quad l \frac{S_2}{cS} = \vec{V} \tag{3}$$

where S –wing surface

S_2 *– horizontal tail surface*

Z_2 *– distance on* O_Z *axis) for neutral point of the horizontal tail*

C_{x2} *–horizontal tail drag coefficient*

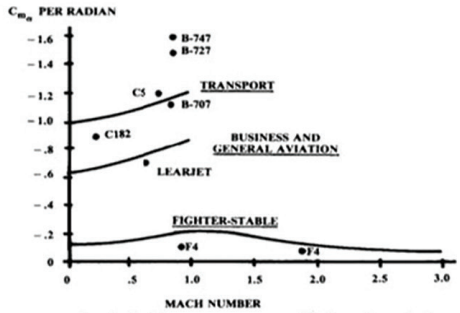

Fig. 5 Typical pitching moment coefficient for airplanes main categories, [10]

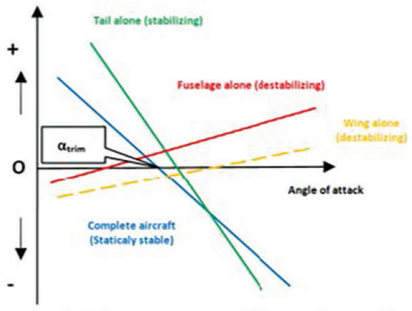

Fig. 6 Pitching moment coefficient values of the building components, [18]

1.2.2. Lateral stability

a. Yaw instability. Ensuring static a yaw stability was not a critical design issue as long as aircraft flight speeds were moderate (subsonic or supersonic speeds). The simple provision of a vertical tail of a surface not too large, arranged behind the aircraft mass center, achieved the condition of static yaw stability, $C_{n_\beta} > 0$, for all flight speeds interval, [9].

For supersonic aircraft, however, with the increase in flight speed, some significant sidesleep flight began to be reported, which in some cases developed unstable lateral movements. The phenomenon is explained by the loss of rotational stability that can occur at high supersonic speeds due to the reduction of the stabilizing moment of the vertical tail in relation to the destabilizing moment of the fuselage (or other elongated hulls outside the aircraft). This trend is more pronounced in aircraft with large elongated fuselages. Indeed the yaw coefficient of stability:

$$C_{n_\beta} = \frac{S_v l_v}{Sb} a_v \left(1 - \frac{d\sigma}{d\beta}\right) - \frac{2kQ}{Sb} \quad (4)$$

where S – *wing lift surface*
b – *span wing*
S_v – *vertical tail surface*
Q – *fuselage volume*
K – *correction factor*
σ – *lateral air deflection*
β – *sidesleep angle*

The coefficient of yaw stability (rotation) is positive as long as the contribution of the vertical tail (the first term in the equation 4) is higher in mode than the contribution of the fuselage (the second term in the equation 4). But with the increase of flight speed a_v decreases and as a result decreases and C_{n_β}, being able to become negative:

$$a_v = \frac{\partial C_z}{\partial \beta} \tag{5}$$

A typical aspect of the variation of the coefficient of the static yaw stability with Mach number is presented in figure 5. The decrease of the static yaw stability is a characteristic phenomenon and the flight at high AoA, as the coefficient of static yaw stability C_{n_β} decreases with increasing AoA. The phenomenon is more pronounced in airplanes with a parasol wing, because the detachments downstream of the wing affect to the vertical tail, which is the main element of the airplane lateral stability, see figure 7.

b. Roll/lateral instability. The condition of static roll/lateral stability is ensured by a negative dihedral effect, $C_{l_\beta} < 0$. During the low AoA of flight, the dihedral effect decreases slowly and linearly with increasing AoA, but for high AoA there is a sudden, destabilizing (positive) variation of the dihedral effect, more pronounced for swept wings aircraft.

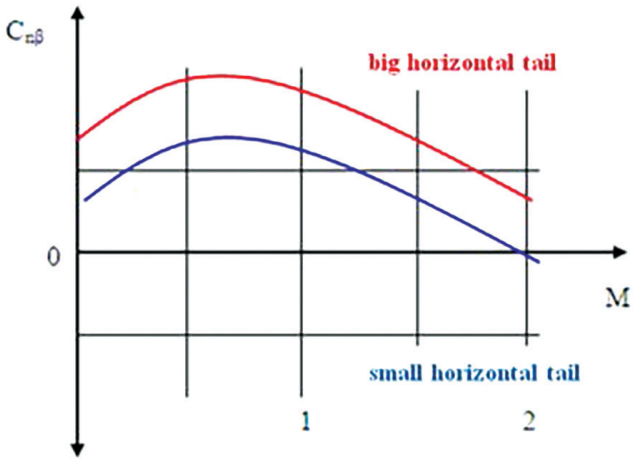

Fig. 7 Yaw stability coefficient versus Mach number

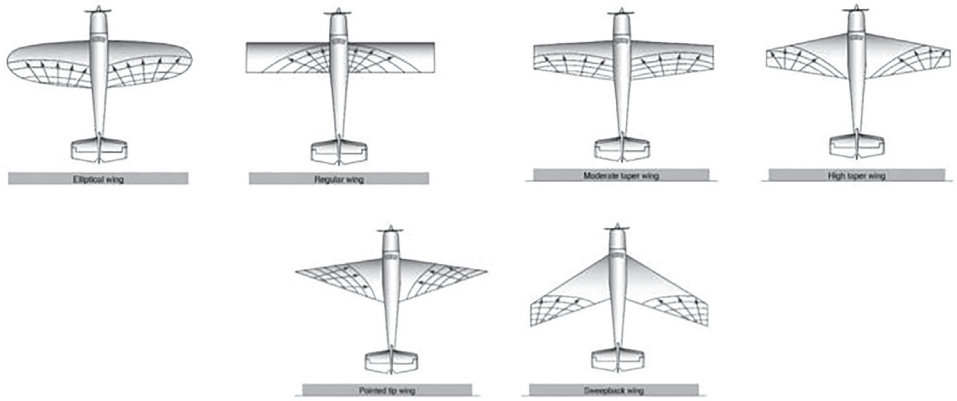

Fig. 8 Boundary layer areas

Figure 8 shows this dependence of the dihedral effect on the AoA. This variation is determined, among other things, by the starting points of the boundary layer, for the straight wing, with low trapezoid, the detachments of the boundary layer begin when the wing is embedded in the fuselage, while on the arrow wing the detachments begin at the extremities.

As a result, the loss of roll stability occurs faster in aircraft with an swep wing. The loss of roll stability, which can occur at high AoA, is extremely dangerous in flights near the ground takeoff and landing - but also in any flight regimes because it can lead to the engagement in aircraft spin flight (see figure 9).

Fig. 9 Roll coefficient stability versus AoA (α), [9]

2. STABILITY ANALYSIS METHOD

XFLR5 freeware applies the method proposed in [15] and the theoretical approach in [16], with this type of analysis, the longitudinal and lateral dynamics are independent and are evaluated separately. According to [12] the software analysis is performed according to: reference axes (solid/vector, geometric and stability); position coordinates; kinetic conditions/rotation vectors and flight conditions. The stability derivatives are calculated according to the equilibrium conditions, and the terminology used refers to the angle of attack (AoA), the glide angle, the UAV mass, the air density, the gravitational acceleration, the lifting surface. The constraints are: air speed, turning radius, (angular) turning speeds, the angular velocities corresponding to the three axes (roll, pitch, and yaw). The analysis procedure involves several steps, according to Figure 10.

The input data required for the analysis are: geometric parameters of the UAV, mass and center of the UAV, parameters defined by the stability analysis, position for the maneuver control (lifting surfaces angles, flap angles), type of flight (with constant speed orconstant turn), see figure 11. The polars graphs can be calculated for different control variables, they are: the lateral angle (around the O_x axis), the pitch angle (around the O_y axis), the flaps angle, the elevator angle, the ailerons angle.

Software analysis provides a number of graph-numerical results, such as: stability and control derivatives, stability derivatives (dimensionless), temporal response, eigenvalues and eigenvectors for longitudinal modes and lateral modes.

From the physical point of view, eigenvalues and eigenvectors represent the natural modes that the plane tends to oscillate, for a standard problem we have for the longitudinal case: two symmetric fugoid modes, two short-period symmetric modes; for the side case: a roll damping mode, a spiral mode, two symmetrical Dutch roll modes.

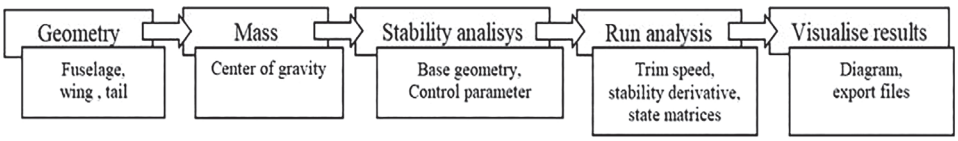

Fig. 10 Stage of stability analysis

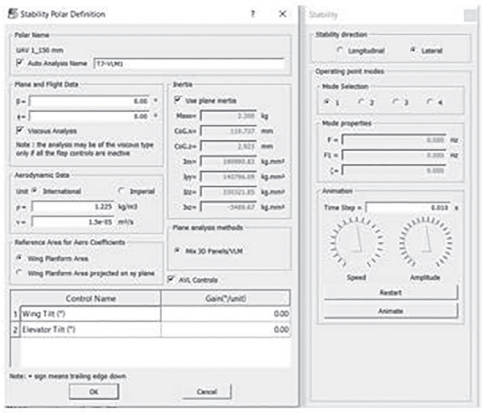

Fig. 11 Input data for stability analysis

3. UAV GEOMETRY

The geometric configuration was made using the Airfoiltools [11] and XFLR5 [12] freeware tools. To visualize the UAV behavior regarding the aerodynamic stability depending on its geometry and mass, we choose a geometric configuration based on two airfoils, NACA 0007 and NACA 2407 (see figure 12), having the characteristics in table 1.

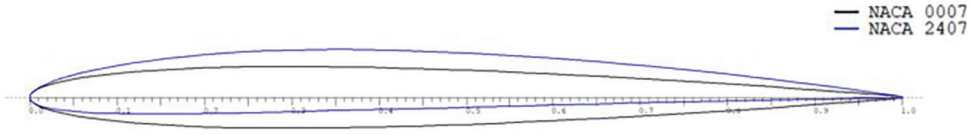

Fig. 12 The airfoils, NACA 0007 and NACA2407.

Table 1. Airfoils characteristics (NACA 0007 and NACA 2407)

Characteristics / profile	NACA 0007	NACA 2407
Chamber	0% for 19,70% Max-x position	2% for 39,50% Max-x position
Max. thickness	7% for 29,1 % Max-x position	7% for 29,1 % Max-x position

The 3D geometries of the UAV (horizontal tail positions) are shown in Figure 13 and having the characteristics in Table 2.

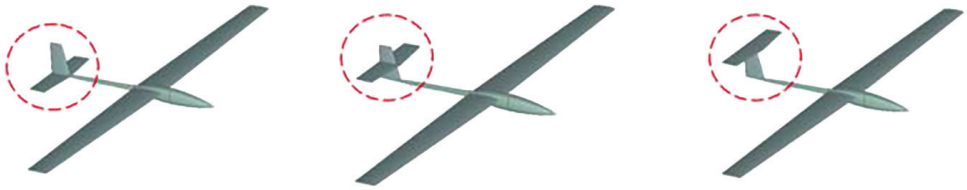

Fig. 13 UAV aerodynamics tail concept

Table 2. UAV features

Characteristics	Value	Characteristics	Value
Span	2000 mm	Taper ratio / Aspect ratio (AR)	1,5 / 16
M.A.C	127 mm	Wing area	25 dm^2
Mass	2,3 kg	Tail volume	0,54

The balancing of the UAV had as a requirement a minimum mass, at the same time it is observed the positioning of the mass of the propulsion system (brushless electric motor and folding propeller - 250 g) together with LiPo batteries (350 g) and radio electronic equipment (autopilot - 200 g) according to figure 14, [13, 14].

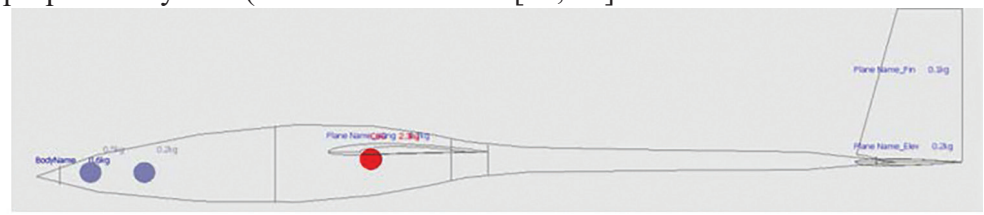

Fig. 14 Balancing of UAV

4. STABILITY ANALYSIS

The stability and control analysis wishes to evaluate the UAV's response to atmospheric disturbances or to those due to maneuver control, under the conditions of constant flight parameters. Grapho-numerical representation is a complex issue that requires some simplifying assumptions (e.g. only small perturbations related to flight conditions are considered), see Table 3, [12, 17]. In order to graphically highlight the stability coefficients (pitch, rotation, roll) and the modes of response to external disturbances, the proposed multicriteria analysis cases are recorded in Table 3.

Table 3. Analysis cases

Balancing cases	130 mm	150 mm			170 mm
Geometrical cases	Horizontal tail down	down	median	up	Horizontal tail up
Perturbation cases	-	1 m/s		2 m/s	-

4.1. Analysis conditions

The initial analysis conditions considered the actual reproduction of the flight parameters for a real UAV geometry (see Table 4).

Table 4. Initial conditions for aerodynamic analysis

Features	Value	Features	Value
Analysis method	Mix 3D panels/VLM	Speed	10 m/s
Air density	1,225 kg/m^3	Boundary conditions	Dirichlet
Iteration	100	VLM method type	Ring vortex VLM2

For the (lateral) stability analysis a number of additional conditions are initiated according to table 5.

Table 5. Initial conditions for the stability analysis

Features	Value	Features	Value
Stability direction	Longitudinal / lateral	Analysis interval	10 s
AoA range	$-5^o \div 5^o$	Sidesleep angle	0^o

4.2. Results and interpretations

a.Balancing cases

The UAV aerodynamic configuration of the analyzed offers for the beginning the variation of the three moment coefficients (pitch - C_m, roll - C_l, yaw - C_n), see figure 15.

The selected balancing cases reveals the following evaluation: according to the variation C_m vs AoA (α) in figure 15a, a self-stable behavior is observed, the longitudinal stability is improved at a previous balancing (170 mm-blue); the rolling coefficient C_l reflects a similar self-stabilizing behavior depending on the increase of AoA> 10^o (figure 15b), similar behavior for all balancing cases, while the variation of the yaw coefficient C_n shows a decrease of stability on the vertical axis depending on the increase of AoA>10^o, similar decrease for all centering cases(figure 15c).

The values of the moment coefficients, compared for AoA = 8^o (critical for NACA 2407) reveal quasi-similar behaviors in terms of stability on the three axes.

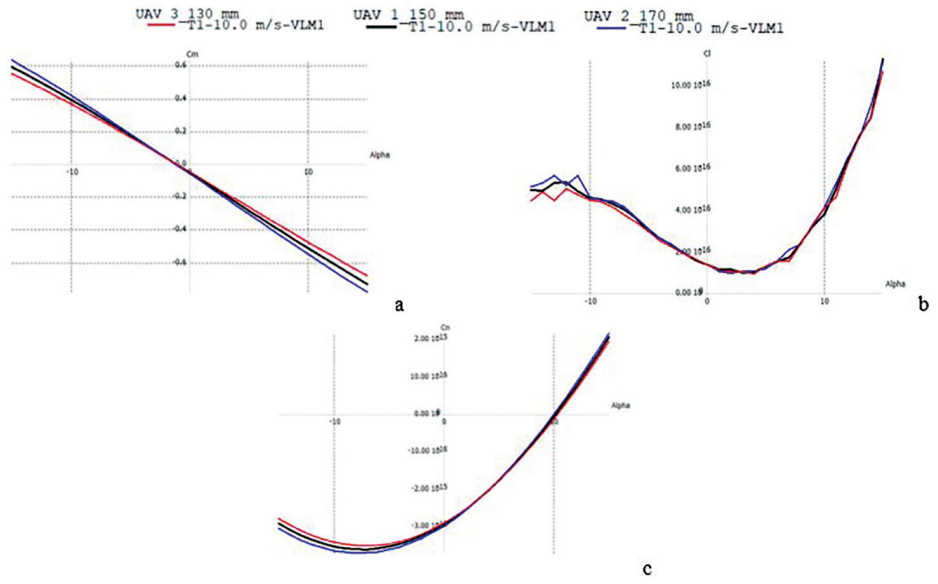

Fig. 15 Variation of moment coefficients versus AoA (a.C_m vs AoA, b. C_l vs AoA) for three balancing cases

b.Geometrical cases

The proposed geometric configurations are analyzed in comparison with the stability coefficients shown in Figure 16. According to Figure 16a a decrease in longitudinal stability is observed with the positioning of the horizontal tail on the height, while the roll coefficient increases to the maximum extrem position of the horizontal tail (Figure 16b), and the yaw coefficient (according to figure 16c) is quasi-constant for the three geometric variants analyzed.

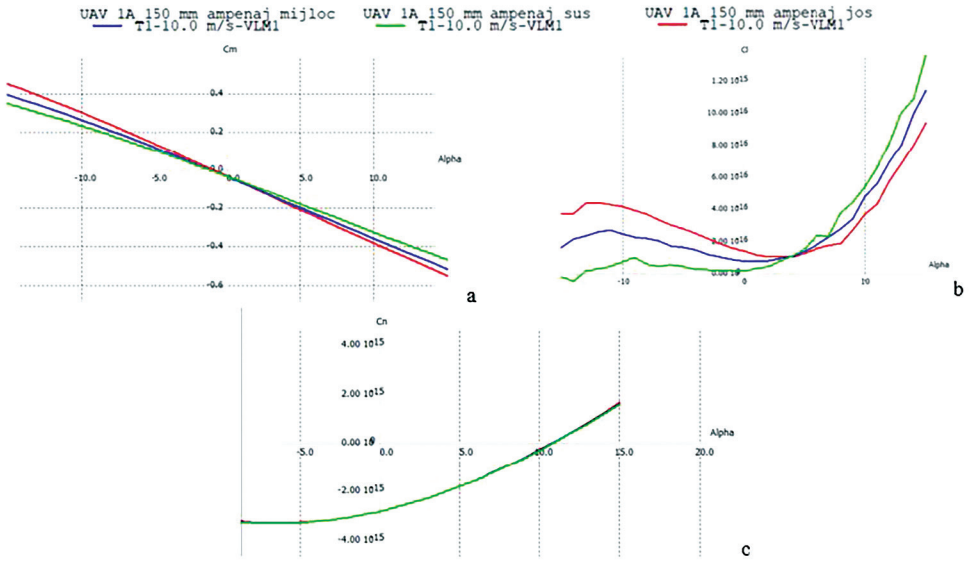

Fig. 16 Variation of moment coefficients versus AoA for the three horizontal tail cases

c. Cases of disturbance

Interpretations of the stability behavior of the UAV relate to the geometric axes, the axes of the UAV and the axes of stability, according to Figure 17.

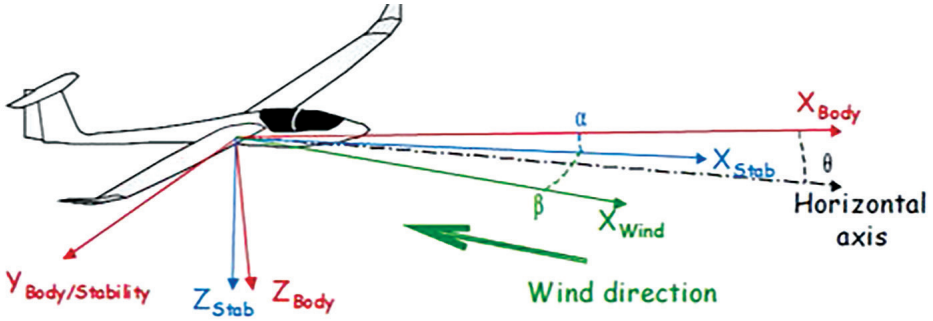

Fig. 17 The UAV axes and stability axes, [12]

The longitudinal stability analysis with balancing for mass center at 150 mm, provides the stability parameters regarding the UAV behavior, as follows: according to figure 18a a damping of the speed variation (*v*) is observed relative to the longitudinal axis (O_x), figure 18b indicates a decrease of the response speed (*w* in m/s) referred to the vertical axis (O_z), figure 18c shows a damping of the drip rate (angle q%) with respect to the lateral axis (O_y).

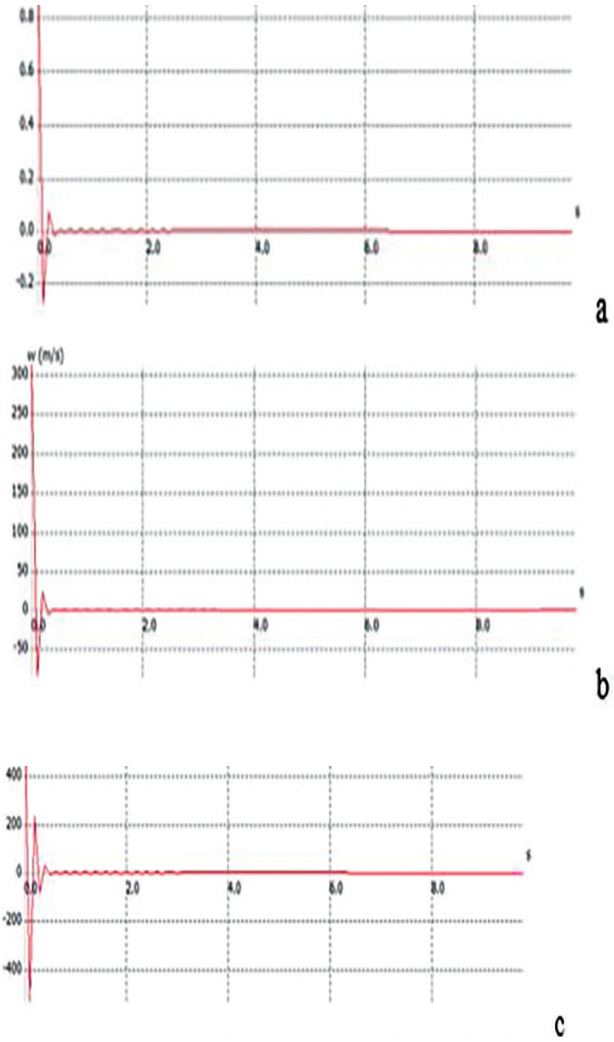

Fig. 18. Varation of kinematic parameters of longitudinal stability

The lateral stability analysis with balancing for mass center at 150 mm provides four relevant parameters for the UAV behavior, as follows: according to figure 19a a damping of the speed variation (*v*) referred to the transverse axis is observed, figure 19b indicates a decrease of the rolling rate (angle p%) referred to the longitudinal axis, figure 19c indicates a decrease in the rate of rotation (angle r%) referred to the vertical axis. As can be seen in Figure 19, the difference in damping values depending on the initial kinetic condition (v = 1 ÷ 2 m / s) of the introduction of the pilot's maneuvering disturbance, damping close to zero values after 8 seconds.

5. CONCLUSIONS

The overall characteristics and performance of the UAV depend directly on the aerodynamic configuration selected from the design phase, aerodynamic and stability analyzes can provide initial data for experimental campaigns in tunnel wind that will confirm or deny the chosen aerodynamic solution.

Stability and control software analysis is an assessment of the response time of a UAV to external disturbances and maneuver report in the case of a flight with constant parameters. The proposed UAV geometry confirms the expectations of the pre-design phase and provides an overview of the analyzed mass and

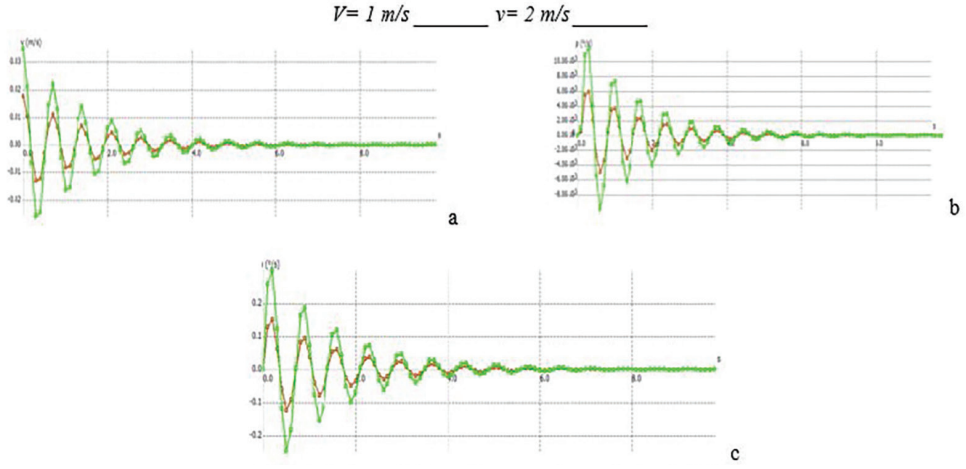

Fig. 19. Varation of kinematic parameters of lateral stability

balancing limits. The XFLR5 analysis tool offers multicriteria possibilities for longitudinal and lateral stability analysis providing relevant numerical data on the response time of the aerodynamic concept transposed in an optimized geometric configuration and centering.

The stability aspects in the case of critical regimes can also be analyzed with the help of CFD numerical codes that are the basis of the established commercial instruments for possible value comparisons of the response parameters.

6. ACKNOWLEDGMENT

This article was made with the support of the documentation approaches within the complex project, acronym MultiMonD2, code PNIII-P1-1.2-PCDDI-2017-0637, contract 33PCCDI / 2018 financed by UEFISCDI.

REFERENCES

[1] Planeaux, J. B. And Barth, T. J., *High angle of attack dynamic behavior of a model high performance fighter aircraft*, AIAA Paper 88-4368, August, 1988

[2] Chapman, G. T. And Tobak, M., *Nonlinear problems in flight dynamics*, NASA-TM-85940, May, 1984

[3] Planeaux, J. B., Beck, J. A. and Baumann, D. D., *Bifurcation analysis of a model fighter aircraft with control augmentation*, AIAA Paper 90-2836, August, 1990

[4] Sibilski, K., & Wróblewski, W. (2012). *Prediction of aircraft spin characteristics by continuation and bifurcation methdos*. In AIAA Atmospheric Flight Mechanics Conference (p. 4799), https://doi.org/10.2514/6.2012-4799

[5] Goman M.G., Khramtsovsky A.V., *Application of continuation and bifurcation methods to the design of control systems*, Phil. Trans. R. Soc., No. A 356, London, 1998, pp 2277-2295

[6] Marusak A. J., Pietrucha J. A., Sibilski K. S., *Prediction of Aircraft Critical Flight Regimes Using Continuation and Bifurcation Methods*, 38th Aerospace Sciences Meeting Technical Papers, USA, 2000, AIAA-2000-0976-CP, American Institute of Aeronautics and Astronautics

[7] Sinha N. K., and Ananthkrishnar N., *Use of the Extended Bifurcation Analysis Method for Flight Control Law Design*, 40th AIAA Aerospace Sciences Meeting, USA, 2002, AIAA-2002-0249-CP, American Institute of Aeronautics and Astronautics

[8] Sibilski K., *Modelling and Simulation of aircraft dynamics of light*, MH, Warsawa, 2005

[9] Reghintovski V., *Fenomene* şi *regimuri critice* în *dinamica* şi *manevrabilitatea aeronavelor militare*, Academia de Inalte Studii Militare, București 1991

[10] Raymer D.P., *Aircraft Design: A Conceptual Approach*, 1989, AIAA education series, ISBN 0-930403-51-7

[11] Airfoil tools, available at http://airfoiltools.com/airfoil/naca4digit

[12] XFLR5, *Analysis of foils and wings operating at low Reynolds numbers*, Guidelines for XFLR5 v6.03, 2011, 71p

[13] Motor electric brushless, available at https://phoenixmodels.ro/ro/motoare-foxy/4888-motor-bl-foxy-c2826-900-masa-171g-kv-900-780w.html

[14] Acumulator LiPo, available at https://phoenixmodels.ro/ro/ray/5258-acumulator-lipo-g4-ray-3250-mah-111v-22650-c.html

[15] James C. Sivells and Robert H. Neely, *Method for calculating wing characteristics by lifting line theory using nonlinear section lift data,* April 1947, NACA Technical Note 1269

[16] B. Etkin and L.D. Reid, *Dynamics of Flight: Stability and Control*. John Wiley and Sons, New York, NY, Third Edition, 1996

[17] Prisacariu V., Cîrciu I., Boşcoianu M., *Flying wing aerodynamic analysis*, Review of the Air Force Academy, 2/2012, Brasov, Romania, ISSN 1842-9238; e-ISSN 2069-4733, p 31-35

[18] Sinem Karatoprak, Serkan Özgen, *Sizing and Optimization of the Horizontal Tail of a Jet Trainer,* 8 The European Conference For Aeronautics and Space Sciences (Eucass), 2019, DOI: 10.13009/EUCASS2019-335, available at https://www.eucass.eu/doi/EUCASS2019-0335.pdf